NAL TR-667T

ISSN 0389-4010
UDC 519.24:
533.6.013.4:
609.7.018.1

TECHNICAL REPORT OF NATIONAL AEROSPACE LABORATORY

TR-667T

New Estimation Method for Flutter or Divergence Boundary from Random Responses at Subcritical Speeds

Yuji MATSUZAKI and Yasukatsu ANDO

April 1981

NATIONAL AEROSPACE LABORATORY

CHŌFU, TOKYO, JAPAN

New Estimation Method for Flutter or Divergence Boundary from Random Responses at Subcritical Speeds*

Yuji MATSUZAKI** and Yasukatsu ANDO**

ABSTRACT

The present paper describes a new technique for estimating the flutter or divergence boundary from responses due to turbulence at subcritical speeds. The boundary can be predicted without estimating or measuring the dampings and frequencies of the aeroelastic modes. The sampled time response is modeled by the mixed autoregressive moving average process. The orders and coefficients of both autoregressive and moving average parts of the process are determined with the aid of Akaike's estimation procedure. The stability boundary is estimated by using Jury's stability determinants which are expressed in terms of the autoregressive coefficients alone. The modal frequencies and dampings are also evaluated from the coefficients. The technique proposed has been applied with success to signals from a cantilever wing model tested in a low supersonic flow. Comparison between the actual and estimated flutter boundaries shows that an accurate estimation can be made from data obtained in a narrow range of the dynamic pressure which is sufficiently below the boundary.

概　　要

従来の様に減衰率と振動数の測定や推定をすることなく，サブクリティカルな領域での気流の乱れによって励振された応答からフラッタ限界値，あるいはダイバージェンス限界値を推定する新しい方法を提案する．離散化した応答は，自己回帰移動平均過程で表わせると仮定し，自己回帰および移動平均過程の次数と係数は赤池の推定法を用いて決定する．限界値の推定は自己回帰係数で表示される Jury の安定行列式を用いて行う．本手法を，当所の遷音速フラッタ試験設備を用いて行った片持翼の試験結果に適用し，限界値より十分低い動圧のデータから精度良くフラッタ限界値の推定が出来ることを明らかにした．

I. INTRODUCTION

Flutter prediction and clearance are very important problems in the design and development of aircraft. Since no analytical prediction can be done with sufficient confidence, it is imperative to verify the flutter clearance both in wind tunnel and in actual flight test. Continuous efforts have been paid in developing accurate, rapid and low cost procedures for forecasting the flutter boundary.[1-3]

Conventional methods for flight flutter testing consist of estimating frequencies and dampings of the aeroelastic modes against the flight speed, and determining the flutter speed mainly with the aid of extrapolation of the damping at subcritical speeds. Since the damping characteristics often change abruptly near the flutter boundary, it is necessary to evaluate them up to speeds which are very close to the boundary. Additionally, dampings are much more difficult to estimate accurately than frequencies. In order to avoid resorting to the damping alone, Zimmerman and Weissenburger[4] proposed a stability para-

* Received, February 25, 1981.

** First Airframe Division.

meter, called as Flutter Margin, which is related to one of the Routh-Hurwitz criteria and shows a more monotonous behavior than damping. This parameter is evaluated from both frequencies and dampings of the two modes. In flight testing, impulsive or harmonic excitation is often used to drive the aeroelastic modes of interest so that the modal response should become large relative to random components caused by turbulence. Usually such an onboard excitation system is costly. For dynamic simulation models tested in wind tunnel, the size or weight of an exciting device is often inadmissible. In addition, the test procedure is time consuming.

An approach which requires no onboard forcing system has recently received widespread attention. The approach is based on analysis of the random response induced by inflight or wind tunnel turbulence, and is classified into two categories: one utilizing classical stochastic theories and the other employing modern system identification techniques.

The power spectral density (PSD) method is a useful tool to estimate the frequency and damping of the vibration modes from noise contaminated data. If the PSD of noise inputs is available, then an accurate estimation can be obtained. However, the PSD of turbulence is not usually measured in the flutter testings. In addition, it is difficult to separate the dampings of two modes if their frequencies are closely spaced. This would be the case when the flight speed is close to the flutter boundary. Another method consists of calculating an ensemble average of segments of the response history, and fitting a decay curve to it. The ensemble average is equivalent to the characteristic response function, provided that the turbulence is uncorrelated. From the fitted decay curve the frequency and damping of the aeroelastic mode are determined. In the United States, this method has widely been applied to flight flutter test[5-7] as well as to wind tunnel tests.[8,9] When the frequencies of the modes are relatively close, analytical difficulties are encountered.[5]

Recent progress in modern system identification techniques which rely heavily on the use of the high speed digital computers is remarkable. In the aeronautical field, such an approach has often been used to extract the aircraft stability and control derivatives from flight test or wind tunnel test data.[10-13] To the authors' knowledge, a paper by Onoda[14] is the first work to apply an identification technique to estimation of the response characteristics of a flutter model. His analysis is based on Akaike's procedure[15] of predictor identification. The stochastic process is given by an autoregressive (AR) model, in which the current value of the process is expressed as a finite, linear combination of its previous values puls a random shock. The finite order of the model is determined by Akaike's final prediction error (FPE) criterion. According to Onoda's numerical result, the estimated orders of the model were about 40 to 60. It is well known[16] that an autoregressive moving average (AR-MA) model, which consists of a linear weighted sum of the shocks (the moving average part) as well as the AR part, may achieve a parsimonous representation. That is, a small number of the orders of AR and MA parts often suffice for the best fit to an actual time series.

As for the AR-MA model, Akaike and his coworkers presented in Ref. 17 an automatic fitting procedure which determines the orders and coefficients of the model for a stationary Gaussian process by minimizing a certain quantity known as Akaike's Information Criterion (AIC). The concept of the procedure is presented in Ref. 18. The usefulness of Akaike's minimum AIC method has been shown in several problems. Application of the procedure appears to be quite effective also to subcritical flutter testings.

In the present paper, we will present a novel technique for predicting the flutter or divergence boundary, which is primarily on a basis of Akaike's procedure and Jury's stability criterion[19] for a linear discrete-time system. The significance of Jury's criterion is that the values of its parameters change in a monotonous manner like the Flutter Margin. The aeroelastic responses

due to wind tunnel turbulence on subcritical conditions are presented by the AR-MA process. In this technique, the stability boundary can be predicted by using only the AR coefficients of the process without measuring or estimating the dampings and frequencies of the aeroelastic modes. In order to demonstrate its effectiveness, the proposed technique is applied to responses of a cantilever wing model which was tested in the Transonic Blowdown Wind Tunnel for Flutter Testing at National Aerospace Laboratory (NAL). The arrangement of this paper is as follows: Section 2 presents a description of the theoretical background of the estimation technique. Section 3 describes the model used and test procedure. Section 4 gives data analysis, results and discussions.

II. THEORETICAL BACKGROUND

The response $\tilde{y}(t)$ of a wing excited by air turbulence on a constant flow condition is sampled at a given interval T to obtain a finite discrete time series $\{y(T), y(2T), \cdots, y(NT)\}$. $y(nT)$ will be simply written as $y(n)$. $\{y(n)\}$ is assumed to be governed by the mixed autoregressive moving average time series model[16]:

$$\sum_{m=0}^{2J} b(m)y(n+m)=\sum_{m=0}^{2J-1} a(m)x(n+m) \tag{1}$$

where $b(0)\neq 0$ and $b(2J)=1$. The order $2J$, the MA coefficients $\{a(m)\}$, and AR coefficients $\{b(m+1)\}$, $m=0, 1, \cdots, 2J-1$, are unknown integer and real numbers to be estimated. A time series $\{x(n)\}$, $n=1, 2, \cdots, N$, represents a noise process to which the system is subjected. The process $\{x(n)\}$ is assumed to be a Gaussian independent random sequence with zero mean and an unknown variance σ^2:

$$E\{x(m)\}=0 \quad \text{and} \quad E\{x(m)x(n)\}=\sigma^2\delta_{mn} \tag{2}$$

where δ_{mn} is the Kronecker delta.

With the sampled data $\{y(n)\}$, $n=1, 2, \cdots, N$, the unknown quantities, J, $\{b(m)\}$, $\{a(m)\}$ and σ^2 can be estimated with the aid of an automatic fitting procedure for the AR-MA model given in Ref. 17. Reference 18 presents details of the concept of Akaike's minimum AIC approach. A set of numerical values of the parameters which minimizes AIC is selected as the best choice. In our problem, AIC is given as

$$[\mathrm{AIC}]=-2\log_e L+8J \tag{3}$$

where L is a likelihood function of a Gaussian process $\{x(n)\}$:

$$L[\{y(n)\}, n=1, \cdots, N;\ J, \sigma^2, \{a(m)\}, \{b(m+1)\}, m=0, \cdots, 2J-1] = \frac{1}{(\sqrt{2\pi}\sigma)^N}\exp\left[-\frac{1}{2\sigma^2}\sum_{n=1}^{N}\{x(n)\}^2\right] \tag{4}$$

Appling the z-transform[19] to Eq. (1), we obtain

$$\sum_{m=0}^{2J} b(m)z^m\left[Y(z)-\sum_{j=0}^{m-1} y(j)z^{-j}\right] = \sum_{m=0}^{2J-1} a(m)z^m\left[X(z)-\sum_{j=0}^{m-1} x(j)z^{-j}\right] \tag{5}$$

where $Y(z)$ and $X(z)$ are, respectively, the z-transforms of $y(n)$ and $x(n)$, i.e.,

$$\begin{aligned}\mathscr{Z}[y]=Y(z)=\sum_{j=0}^{\infty} y(j)z^{-j}\\ \mathscr{Z}[x]=X(z)=\sum_{j=0}^{\infty} x(j)z^{-j}\end{aligned} \tag{6}$$

Hence, the transfer function is given by

$$H(z)=\sum_{m=0}^{2J-1} a(m)z^m \Big/ \sum_{m=0}^{2J} b(m)z^m, \tag{7}$$

whence we obtain the characteristic equation:

$$\sum_{m=0}^{2J} b(m)z^m=0 \tag{8}$$

Let us now discuss briefly the stability of a linear discrete-time system.[19] Like in the continuous-time case, the system is defined to be stable if to all bounded inputs there always correspond bounded outputs. This is satisfied if and only if all the singularities of the transfer function lie inside the unit circle. Since the numerator of Eq. (7) is regular, the present system is stable as long as

$$|z_m|<1 \quad \text{for } m=1, \cdots, 2J \quad (9)$$

where z_m's are the roots of the characteristic equation given by Eq. (8). For actual estimation of the stability, Jury's determinant method,[19] which is similar to the Routh-Hurwitz criterion for the continuous system, is suitable. For the characteristic polynomial which is presented by

$$G(z)=\sum_{m=0}^{n} c(m)z^m=0 \quad (10)$$

with n being an even number and $c(n)>0$, the stability conditions[19] are as follows:

$$G(1)>0, \quad G(-1)>0 \quad (11)$$

$$F^{\pm}(m)=|X_m^* \pm Y_m^*|>0 \quad \text{for } m=1, 3, \cdots, n-1 \quad (12)$$

where X_{n-1}^* and Y_{n-1}^* are $(n-1)\times(n-1)$ matrices defined by

$$X_{n-1}^*=\begin{bmatrix} c(n) & c(n-1) & \cdots & c(3) & c(2) \\ 0 & X_{n-3}^* & c(n) & c(n-1)\cdots c(4) & c(3) \\ & & 0 & c(n) \quad \cdots c(5) & c(4) \\ \vdots & & \vdots & & \vdots \\ & & 0 & \cdots\cdots\cdots\cdots 0 \; c(n) & c(n-1) \\ 0 & \cdots\cdots\cdots\cdots\cdots\cdots\cdots\cdots & & & c(n) \end{bmatrix} \quad (13.1)$$

$$Y_{n-1}^*=\begin{bmatrix} c(n-2) & c(n-3) & \cdots & c(1) & c(0) \\ c(n-3) & \cdots\cdots\cdots & & c(0) & 0 \\ \vdots & & & & \vdots \\ c(0) & 0 & \cdots\cdots\cdots\cdots & & 0 \end{bmatrix} \quad (13.2)$$

X_{n-1-2k}^* and Y_{n-1-2k}^* are $(n-1-2k)\times(n-1-2k)$ matrices which are obtained by deleting the first k rows and columns and the last k rows and columns from X_{n-1}^* and Y_{n-1}^*, respectively. They are called inners of X_{n-1}^* and Y_{n-1}^*, respectively. $F^{\pm}(m)$ are the determinants of matrices $[X_m^* \pm Y_m^*]$.

Hence, the stability boundary can be defined as the lowest flow speed for which at least one of Eqs. (11) and (12) is violated. In other words, the boundary is, for example, the minimum flow speed at which

$$G(1)=0, \; G(-1)=0, \quad \text{or} \quad F^{\pm}(m)=0 \quad \text{for } m=1, 3, \cdots, n-1 \quad (14)$$

To predict such a speed, we will evaluate the stability parameters, $G(1)$, $G(-1)$, and $F^{\pm}(m)$ at several subcritical speeds, plot the stability parameters against the flow speed, and fit a curve to points of each stability parameter. Intersecting points of the curves with the flow speed coordinate would represent the speeds at which Eqs. (14) are satisfied.

Next, let us describe the calculation of ω_m and η_m with the use of the estimated AR coefficients, and the relation between Jury's and Routh-Hurwitz's stability criteria. We assume here that the response characteristics are expressible in terms of an oscillatory motion of a viscously damped J-degree-of-freedom system whose response $\tilde{y}(t)$ is given by

$$\tilde{y}(t)=\sum_{m=1}^{J}\{A_m \exp(s_m t)+B_m \exp(\bar{s}_m t)\} \quad (15)$$

In Eq. (15), $\bar{s}_m$ is the complex conjugate of s_m, and

$$s_m=\{-\eta_m+i(1-\eta_m{}^2)^{1/2}\}\omega_m \quad (16)$$

where ω_m and η_m represent, respectively, the frequency and damping ratio of the m-th mode. If $\eta_m{}^2 \ll 1$, then Eq. (16) reduces to

$$s_m=(-\eta_m+i)\omega_m \quad (17)$$

Hence, we have

$$\omega_m=\text{Imag}(s_m) \quad (18.1)$$

$$\eta_m=-\text{Real}(s_m)/\text{Imag}(s_m) \quad (18.2)$$

The characteristic equation of this corresponding system, represented by

$$\sum_{m=0}^{2J} C_m s^{2J-m}=0, \quad C_0=1, \quad (19)$$

possesses J pairs of complex conjugate roots, s_m and $\bar{s}_m$, for $m=1, 2, \cdots, J$. That is, Eq. (19) is rewritten as

$$\prod_{m=0}^{J}(s-s_m)(s-\bar{s}_m)=0 \quad (20)$$

There is a relationship between the z- and s-variables which is given by[19]

$$z=\exp(sT) \tag{21}$$

Using Eq. (21), we may calculate s_m and $\bar{s}_m$ since z_m's and $\bar{z}_m$'s for $m=1, 2, \cdots, J$, are evaluated numerically from Eq. (8) where $b(m)$'s have been estimated. Then, substituting s_m and $\bar{s}_m$ into Eqs. (18) or (16), we obtain ω_m and η_m.

Substitution of s_m's and $\bar{s}_m$'s into Eq. (20) and comparison of Eq. (19) with Eq. (20) determine the coefficients $\{C_m\}$ in Eq. (19). Therefore, the stability boundary of the aeroelastic system can be examined also with the aid of the Routh-Hurwitz criterion in the same way as for Jury's determinant method. The stability conditions for the characteristic equation presented by Eq. (19) are as follows[20]:

$$C_m>0 \quad \text{for } m=0, 1, \cdots, 2J$$
and
$$D_m>0 \quad \text{for } m=1, 2, \cdots, 2J \tag{22}$$

where

$$D_m=\begin{vmatrix} C_1 & C_0 & 0 & 0 & 0 & \cdots\cdots \\ C_3 & C_2 & C_1 & C_0 & 0 & \cdots\cdots \\ C_5 & C_4 & C_3 & C_2 & C_1 & \cdots\cdots \\ \vdots & \vdots & \vdots & \vdots & \vdots & \vdots \\ C_{2m-1} & C_{2m-2} & \cdots\cdots & \cdots\cdots & \cdots\cdots & C_m \end{vmatrix} \tag{23}$$

In each determinant, all C's with negative subscripts or with subscripts greater than $2J$ are to be replaced by zero. It is well known that the condition defined by

$$C_{2J}=0 \tag{24}$$

determines the boundary for static instability or divergence. On the other hand, the critical condition for aperiodicity in the z-plane is given by[21]

$$G(1)=0 \tag{25}$$

or

$$G(0)=c(0)=0 \tag{26}$$

However, only Eq. (25) governs the static instability.

III. MODEL AND TEST PROCEDURE

In order to obtain the data to which the proposed technique is applied, a test was conducted by using a cantilever wing model in the transonic blowdown tunnel at NAL which has the 0.6×0.6 m test section. The wing used had a length of 137 mm normal to the flow direction, angle of sweep of 45°, aspect ratio of 4, taper ratio of 0.657, and the airfoil was NACA65A004. The responses to wind tunnel turbulence were measured through a pair of strain gauges which were glued at the same positions on the upper and lower surfaces of the wing. In vibration test, several other gauges were also used in order to find a combination of gauge's position and orientation which would ensure a simultaneous measurement of aeroelastic modal responses associated with the first three natural modes. Fig. 1 shows the wing configuration,

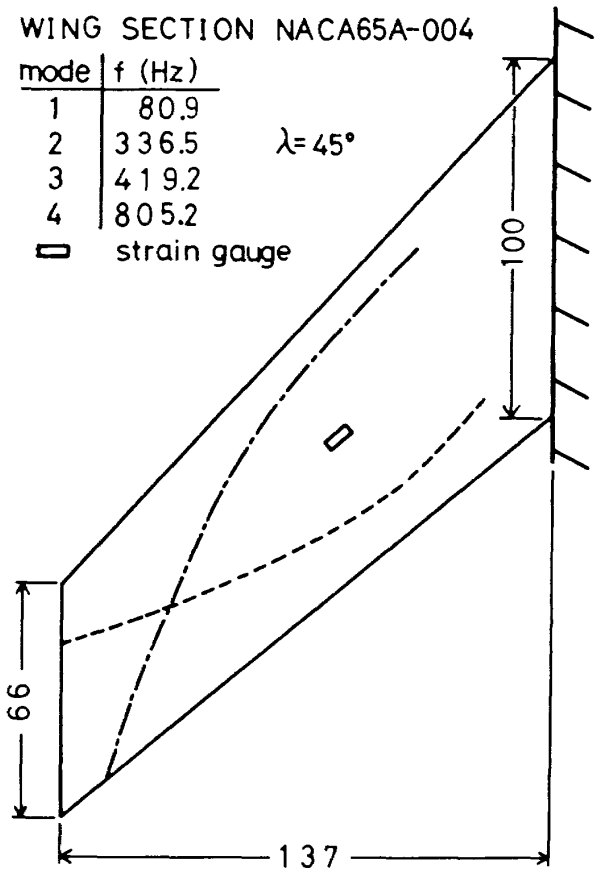

Fig. 1 Wing configuration, strain gauge's location and the first four natural frequencies. Nodal line: 2nd mode (- - - - -), 3rd mode (—— - —— -)

strain gauge position, the first four natural frequencies and nodal lines of the second and third modes. The nodal line of the first mode was located at the clamped edge of the model.

With the Mach number being fixed at $M=1.17$, the measurement of the response was made at twelve dynamic pressures above $Q=0.5$ kg/cm², which was the minimum pressure attainable at this Mach number. At each dynamic pressure the signals of the response were recorded for about 10 seconds on a FM magnetic recorder. The critical dynamic pressure, Q_f, at which flutter started to occur actually in the test was 0.97 kg/cm². Fig. 2 illustrates a typical example of strain gauge signal $\tilde{y}(t)$ at 78% of Q_f.

Fig. 2 A typical strain guage signal at $Q=78\%\ Q_f$

IV. DATA ANALYSIS AND RESULTS

Before discrete time series $\{y(n)\}$ were generated by sampling the signals, they were narrowed by a band pass filter to the frequency range of interest. Two ranges of frequency were used: one included the first two natural frequencies but excluded the third and higher ones, and the other contained the first three alone. Let us describe both cases separately.

1). Two-Mode Analysis

The upper and lower frequencies of the filter were set to 70 and 350 Hz, respectively, since the first two natural frequencies were 80.9 and 336.5 Hz. After a preliminary examination was made for a number of combinations of values of sampled interval T, number of data points N and the maximum lag of covariance k_{max}, used in Akaike's procedure, the data analysis was carried out with $T=200\,\mu$sec, $N=20{,}000$ and $k_{max}=200$. This means that 4 seconds' response was analyzed at each dynamic pressure. For all the signals, the estimated order of the AR part by Akaike's minimum AIC procedure is fourth. That is, the system which corresponds to the signals filtering has two degrees of freedom. The estimated values of the AR coefficients and stability parameters* $G(1)$, $G(-1)$, $F^{\pm}(3)$ at twelve dynamic pressures are, respectively, given on Tables 1 and 2.

It is seen that, among the stability parameters, $F^{-}(3)$ predicts the stability boundary. Since $G(1)$ is not considered to become negative for a pressure range which is above and close to the highest dynamic

* Since $F^{+}(1)=1+b(0)$, they are not tabulated.

Table 1 Estimated values $\{\hat{b}(m)\}$ of the characteristic polynomial, Eq. (8), with $b(4)=1$

Q(kg/cm²)	Q/Q_f[a]	$\hat{b}(3)$	$\hat{b}(2)$	$\hat{b}(1)$	$\hat{b}(0)$
0.53	0.55	−3.738	5.360	−3.495	0.8755
0.53	0.55	−3.742	5.373	−3.510	0.8815
0.59	0.61	−3.737	5.361	−3.499	0.8781
0.64	0.66	−3.755	5.403	−3.530	0.8851
0.67	0.69	−3.752	5.393	−3.519	0.8809
0.75	0.77	−3.740	5.373	−3.512	0.8828
0.76	0.78	−3.736	5.360	−3.498	0.8779
0.80	0.82	−3.734	5.342	−3.467	0.8625
0.83	0.86	−3.767	5.443	−3.572	0.8999
0.84	0.87	−3.749	5.393	−3.523	0.8835
0.86	0.89	−3.766	5.447	−3.582	0.9053
0.90	0.93	−3.783	5.494	−3.625	0.9183

a) Q_f: Actual flutter boundary (0.97 kg/cm²)

Table 2 Jury's stability parameters[a]

Q(kg/cm²)	$G(1)$	$G(-1)$	$F^+(3)$	$F^-(3)$
0.53	0.2827×10^{-2}	14.46	0.8167×10^{-1}	0.2274×10^{-4}
0.53	0.2784	14.50	0.8022	0.2193
0.59	0.3273	14.48	0.8260	0.1785
0.64	0.3010	14.57	0.7109	0.1143
0.67	0.3070	14.55	0.7060	0.1200
0.75	0.4092	14.51	0.7453	0.1067
0.76	0.3970	14.47	0.7870	0.1173
0.80	0.3502	14.41	0.7305	0.1006
0.83	0.3898	14.68	0.5727	0.04464
0.84	0.4008	14.55	0.6450	0.05792
0.86	0.4544	14.70	0.5588	0.02313
0.90	0.4225	14.82	0.4466	0.02095

a) $F^{\pm}(1)=1\pm b(0)$ are not given.

pressure, we may conclude that the instability observed should not be of divergence type. The values of the determinant $F^-(3)$ are plotted by circles against the dynamic pressure in Fig. 3. The least squares method is used to fit a straight line to the circles given only at the lowest seven dynamic pressures, that is, at 55 to 78% of Q_f. The part of extrapolation is indicated by a broken line. In this case, the estimated critical dynamic pressure $\hat{Q}_f$ which is given by the intersecting point of the broken line with the horizontal coordinate is 97.4% of Q_f. For comparison, the measured critical dynamic pressure is shown by a mark, $\times$, on the coordinate. Agreement between the actual flutter boundary and estimated one is quite good even though the estimation was made by using the data in a pressure range which was far from the boundary.

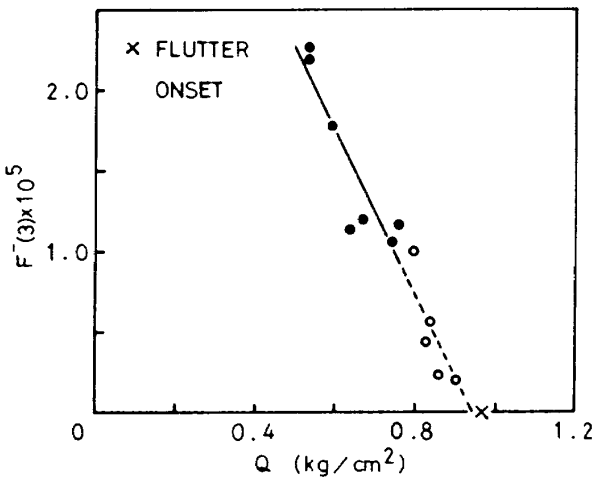

Fig. 3 $F^-(3)$ and estimation of flutter boundary: straight-line fitting to the lowest seven dynamic pressures

In order to examine the change in accuracy of the estimation with increasing data points, the first row in Table 3 presents the values of the estimated-to-actual pressure ratio (%) which were calculated by changing the number of the points, K, from six to twelve. The estimation was repeated by adding, each time, one point at the pressure which is next to the highest pressure in the previous set of the points. The estimated values $\hat{Q}_f$ coincide with the measured value Q_f very well, if at least seven points in the lower pressure range are used. As an aid in judging how the line fits the stability parameter $F^-(3)$, we present at the second row of Table 3 the normalized standard deviation, which is defined by

$$S.D.=\left[\sum_{j=1}^{K}\{f_c(j)-f(j)\}^2/K\{f(1)\}^2\right]^{1/2}\times100 \tag{27}$$

In Eq. (27), $f(j)$ and $f_c(j)$ denote, respectively, $F^-(3)$ at the j-th dynamic pressure and the corresponding value which is calculated from a fitted line. Satisfactory fits to straight lines were obtained.

Figures 4a and 4b illustrate the frequencies f_m and dampings η_m of the aeroelastic modes which were evaluated by using the AR coefficients. The results associated with the first and second modes

Table 3 Comparison of estimated flutter boundaries ($\hat{Q}_f/Q_f$) and normalized standard deviations (S.D.) of the straight-line fitting

No. of data, K		6	7	8	9	10	11	12
Q/Q_f range (from 0.55)		~0.77	~0.78	~0.82	~0.86	~0.87	~0.89	~0.93
Jury[a]	$\hat{Q}_f/Q_f$ (%)	91	97	101	98	98	97	97
	S.D. (%)	8.2	9.4	9.3	9.3	8.8	8.8	8.4
Routh-Hurwitz[b]	$\hat{Q}_f/Q_f$	91	97	102	98	98	97	97
	S.D.	8.4	9.6	9.6	9.6	9.1	9.1	8.7
Flutter Margin[c]	$\hat{Q}_f/Q_f$	94	99	99	99	99	99	100
	S.D.	7.6	8.2	7.7	7.2	6.9	6.7	6.8

a) $F^-(3)$, b) D_3, c) D_3^m

are indicated by circles and triangles, respectively. For comparison, the frequencies of the first two modes obtained from the vibration test in still air are given at $Q=0$ in Fig. 4a. It should be noted that they

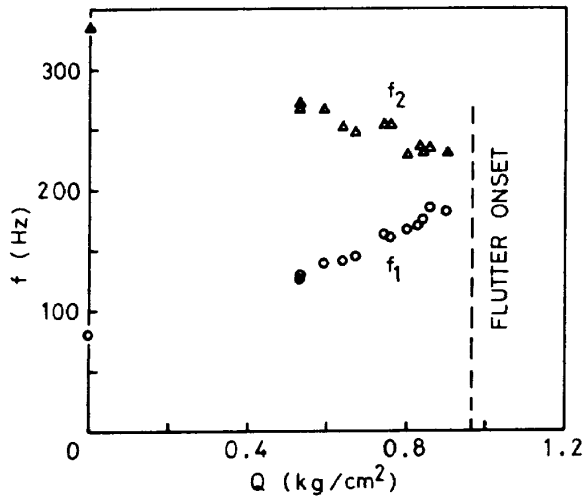

Fig. 4a Estimated frequencies vs. dynamic pressure

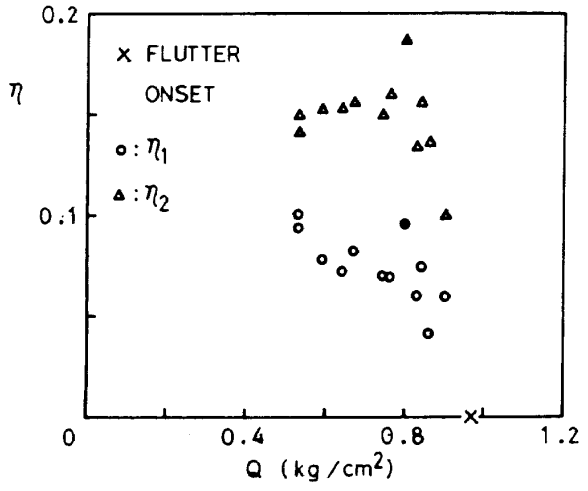

Fig. 4b Estimated damping ratios vs. dynamic pressure

are not necessarily equivalent to the values which would be measured by decreasing the dynamic pressure down to zero while the Mach number is fixed at $M=1.17$. As has been expected, the two frequencies approach as the dynamic pressure increases, and they are closely spaced near the flutter boundary. Dispersion of the estimated frequencies is rather small.

According to the experimental result of a wing in a low subsonic flow presented in Ref. 22, measured values of damping spread widely above a certain flow speed. In the present case, the estimated values of the damping versus the dynamic pressure are less scattered than expected. This is considered to be because each estimation was made in an average sense for the response of 4 seconds. In Fig. 4*b*, a cross on the coordinate represents the actual flutter boundary where at least one of the damping ratios is expected to have vanished. Both the damping ratios at $Q=0.80$ kg/cm^2 are remarkably high compared with others. Let us exclude these points in the following discussion. The damping of the first mode represented by circles seems to decrease with increasing dynamic pressure in the range tested. On the other hand, as the pressure increases, that of the second mode given by triangles is considered to increase gradually to the maximum value which is attained near the pressure $Q=0.80$ kg/cm^2 (82% Q_f), and to go down very sharply with further increase in the pressure. This damping ratio appears to become negative above the critical dynamic pressure. It is evident that an accurate prediction of the

Table 4 Routh-Hurwitz' determinants and Flutter Margin

Q (kg/cm²)	D_1 (1/sec)	D_2 (1/sec³)	D_3 (1/sec⁶)	D_4 (1/sec¹⁰)	D_3^m (1/sec⁴)
0.53	0.6650×10^{3}	0.1612×10^{10}	0.4435×10^{18}	0.8472×10^{30}	0.1003×10^{13}
0.53	0.6309	0.1569	0.4235	0.7941	0.1063
0.59	0.6497	0.1623	0.3468	0.7660	0.08216
0.64	0.6102	0.1375	0.2189	0.4424	0.05877
0.67	0.6338	0.1374	0.2316	0.4785	0.05763
0.75	0.6232	0.1448	0.2058	0.5669	0.05298
0.76	0.6512	0.1542	0.2283	0.6117	0.05382
0.80	0.7394	0.1460	0.2002	0.4767	0.03661
0.83	0.5268	0.1077	0.08354	0.2169	0.03010
0.84	0.6191	0.1245	0.1114	0.3002	0.02907
0.86	0.4972	0.1041	0.04293	0.1297	0.01737
0.90	0.4260	0.08134	0.03798	0.1059	0.02092

boundary from information of the damping alone is a quite difficult task even though all the data up to the highest pressure are taken into account.

Next, let us briefly examine the results which were obtained by using the Routh-Hurwitz criterion. In this case, the flutter boundary was determined by extrapolation on D_3. Table 4 gives the values of the Routh-Hurwitz determinants* as well as those of a modified parameter D_3^m which is defined by

$$D_3^m = D_3/C_1^2 \qquad (28)$$

The modified determinant is equivalent to the stability parameter (Flutter Margin) which was proposed with the use of parabolic extrapolation in Ref. 4. It is noted that these determinants are evaluated from the AR coefficients. The critical pressures estimated with the aid of the straight-line fitting to D_3 and D_3^m are also presented for $K=6$ to 12 in Table 3. As mentioned in Section 2, D_3 and $F^{-}(3)$ are related with directly. Their corresponding values of the flutter boundary and standard deviation agree with each other. It is remarkable that the straight-line extrapolation on D_3^m predicts the flutter boundary within one percent error for $K\geq7$. For the system with more than two degrees of freedom, however, there appears to be no appropriate modification of the Routh-Hurwitz stability parameters given by Eqs. (22). As for a parabolic extrapolation on $F^{-}(3)$, D_3 and D_3^m, it did not work as well as the straight-line fitting.

In the above discussion, the accuracy of the estimated flutter boundaries can be examined by comparing the measured value. However, as for the modal frequencies and, especially, dampings, it was difficult to extract reliable values from the signals by other methods. Regarding the application of the AR model to the signals, the orders of the model were estimated by Akaike's FPE criterion[15] to be more than 40 as in Onoda's case[14]. Its numerical result was used to make the PSD estimation[15,23] as a preparatory study for the AR-MA model analysis. The Random Decrement approach was also applied to the sampled signals to generate oscillatory decay curves. However, the use of the least squares method given in Ref. 24 was unsuccesful in separating the two modes. Hence, there is no appropriate set of data to be compared with the estimated values of both damping and frequency given by the present technique. In the appendix of this paper, therefore, we shall examine the accuracy of estimation of the damping and frequency by using numerical models.

2). Three-Mode Analysis

In the preceeding, two aeroelastically predominant modes are well separated from other modes. However, this is not always the case. Now we will examine the applicability of this flutter prediction method

* The coefficients $\{C_m\}$ are not tabulated since none of them gives the stability boundary.

to signals which contain more than two modes. The signals were processed by the band pass filter with the upper and lower frequencies being set to 70 and 450 Hz, respectively. In addition to the first two modes, the signals were expected to include only the third mode. For the sampled signals, however, Akaike's minimum AIC method indicated that the orders of the best fitted AR-MA model were about 10 to 20. That is, the model represented a system with 5 to 10 degrees of freedom. Since the estimated orders of the model and, consequently, the maximum orders of Jury's determinant were too large to predict the flutter boundary efficiently, Akaike's program was modified such that the determination of the AR and MA coefficients was made only for given orders without searching for the minimum value of his information criterion. All the analyses were carried out with the orders of AR and MA parts being fixed at 8 and 7, respectively, for $N=20{,}000$, $T=400\,\mu$sec and $k_{max}=200$.

The stability boundary was determined by the determinant $F^{-}(7)$. In Fig. 5, its values are plotted by solid and open circles against the dynamic pressure. The circles in the lower half of the pressure range are quite scattered but those in the upper half appear to be consistent. Figs. 6a and 6b show the frequencies and dampings, respectively. In Figs. 5 and 6, the actual flutter boundary is indicated like in Figs. 3 and 4. The first three natural frequencies are given on the ordinate in Fig. 6a. Examining the results of Figs. 6 carefully, it seems to be reasonable to omit the data at the lowest third and fourth pressures, since the estimated frequencies or dampings indicated by solid marks are deviated greatly from others. If doing so, it is obvious that Fig. 5 is still very useful in indicating the stability margin. As for the frequencies, two modes are estimated to exist between about 400 and 460 Hz. Since the upper frequency of the band pass filter is 450 Hz, the mode of the higher frequency is considered to be a ghost or fictitious mode[25] which originates in the course of data processing. Comparing with the results given in Figs. 4a and 4b, agreement between the corresponding first two frequencies is good, but the dampings are much higher in the three-mode analysis than the corre-

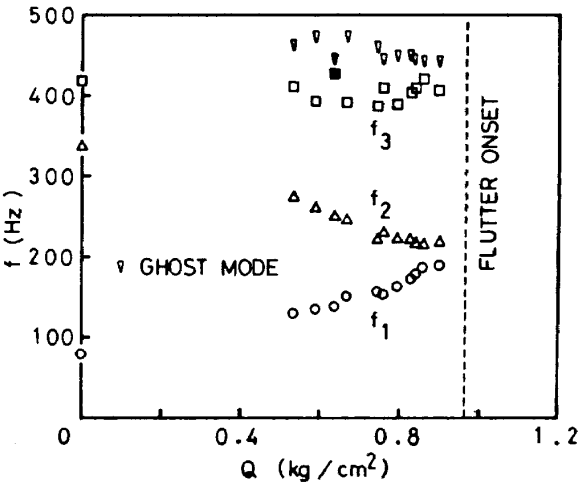

Fig. 6a Estimated frequencies vs. dynamic pressure

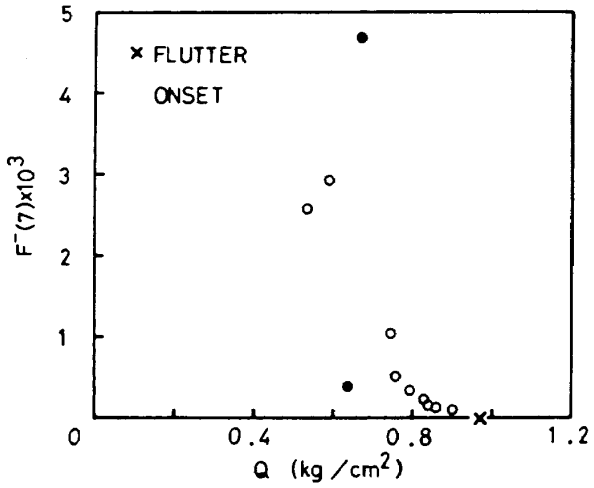

Fig. 5 $F^{-}(7)$ vs. dynamic pressure

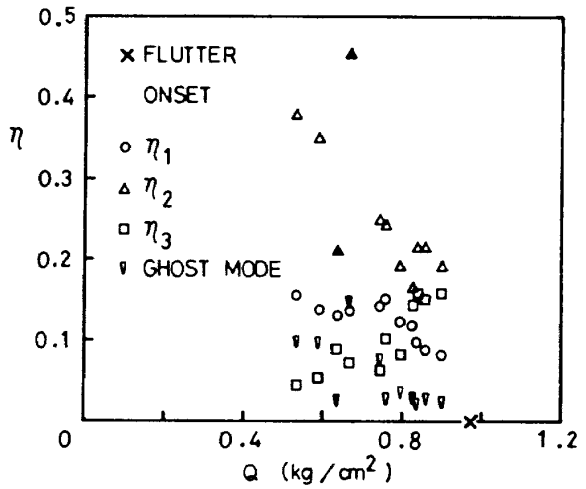

Fig. 6b Estimated damping ratios vs. dynamic pressure

sponding ones in the two-mode analysis. It is evident that this estimation technique of the flutter boundary is quite effective even for the signals which contain more than two degrees of freedom, as is seen in Fig. 5 where the solid circles are neglected.

Using the simple aeroelastic wing model, we have presented a basic concept on which the computer-oriented and practical approach of flutter prediction may be built. Let us summarize the superior points of the present technique over other methods. In existing methods, estimation or measurement of the modal dampings is prerequisite for prediction of the flutter boundary. An accurate evaluation of the dampings is, however, the most difficult task in many occasions. This is also true for the present estimation procedure, as shown by comparison between the results of the two- and three-mode analyses, and in the appendix. Hence, instead of using the damping ratios, this prediction technique determines the flutter boundary on a basis of the autoregressive coefficients of the time series model which represents the response of the wing, since the coefficients can be estimated more accurately than the damping ratios. Another advantage of the technique is that Jury's stability determinants evaluated in terms of the coefficients show monotonous characteristics with increasing flow speed, even when the signals treated contain more than two degrees of freedom.

The flutter prediction in actual flight testing could be done without excessive difficulty. Further refinements in data processing, and expansions of applicability and reliability of the technique are being attempted through a wind tunnel test in a moderate supersonic flow and a flight test at NAL.

V. CONCLUDING REMARKS

A new estimation method on flutter or divergence boundary from subcritical responses due to turbulence has been proposed. The response is represented by the mixed autoregressive moving average process. The flutter prediction is based on Akaike's estimation procedure and Jury's stability criterion on the discrete-time system. Demonstration of the method is presented by using the response signals of a cantilever wing to wind tunnel turbulence in a low supersonic flow. Comparing with the actual flutter boundary, we conclude that the method proposed can predict the flutter boundary quite accurately from the signals which were measured in a narrow dynamic pressure range being sufficiently below the boundary. The method is effective even for the signals containing more than two aeroelastic modes.

ACKNOWLEDGEMENT

The authors would like to express their sincere thanks to Dr. H. Akaike of the Institute of Statistical Mathematics, Tokyo, for his invaluable comments on the application of his minimum AIC procedure. They acknowledge the assistance of Messrs. H. Ejiri and T. Kikuchi of the First Airframe Division.

APPENDIX: APPLICATION OF THE ESTIMATION TECHNIQUE TO NUMERICAL MODELS

In the text of the present paper, the estimation technique has been used to determine the orders and coefficients of the AR-MA representation and the modal frequencies and dampings. Here, we examine the accuracy of the estimation, and the data processing to find a more effective use of the technique for future applications, by using numerical models of a system with two degrees of freedom whose frequencies are spaced more closely than in the flutter model of the text.

The signals to be used for estimation is a response of the system subjected to a sequence of random impulsive forces. If a unit impulse is applied at $t=0$ to a single mode with frequency f_j and damping ratio η_j, then its response $h_j(t)$ is expressible by

$$h_j(t)=a_j \exp(-2\pi\eta_j f_j t)\sin[2\pi(1-\eta_j^2)^{1/2}f_j t] \quad \text{for } t<0 \quad (A1)$$
$$=0$$

where a_j is a constant. Hence, sampling at an interval T, we obtain a finite discrete

time series $\{h(n)\}$, $n=0, 1, \cdots, N-1$, of the response of the system with two degrees of freedom:

$$h(n)=\sum_{j=1}^{2} a_j \exp(-2\pi\eta_j f_j nT) \times \sin[2\pi(1-\eta_j^2)^{1/2} f_j nT] \quad \text{for } n<0 \qquad (A2)$$
$$=0$$

provided that the system is motionless until the input is applied. Let us assume that the impulses are given at a constant interval mT, but are uncorrelated in its magnitude with zero mean and variance of unity. That is, if the inputs are sampled at the same interval as for the response, we have a sequence of the inputs $\{I(n)\}$, $n=0, 1, \cdots, N-1$, where

$$I(n)\neq 0 \quad \text{for } n=km,\ k=0, 1, \cdots \qquad (A3)$$
$$=0 \quad \text{for } n\neq km$$

with $E\{I(n)\}=0$ and $E\{I(im)I(jm)\}=\delta_{ij}$

Then, the finite time series $\{y(n)\}$, $n=0, 1, \cdots, N-1$, of the total response of the system due to all the previous inputs are witten as

$$y(n)=\sum_{k=0}^{n-1} I(k)h(n-k) \qquad (A4)$$

The time series $\{y(n)\}$ are generated for two different combinations of f_1 and f_2, that is, Case I: $f_1=190$ and $f_2=210$ Hz, and Case II: $f_1=195$ and $f_2=205$ Hz. A typical set of other parameters used is: $N=4096$, $a_1=a_2=1$, $\eta_1=\eta_2=0.01$, $T=1$ msec and $m=8$. For the given set of f_j's and η_j's. the corresponding AR coefficients $\{b(n)\}$, $n=0, \cdots, 4$, are determined by using Eqs. (16), (21) and (8). Before the estimation technique is applied to the time series $\{y(n)\}$, they are processed through digital band pass filtering to limit their frequency range. The upper and lower frequencies, f_U and f_L, of the filtering are chosen in this example such that $f_L=f_1-20$ and $f_U=f_2+20$ Hz. Since Akaike's minimum AIC procedure estimates AR's order to be fifth for the signals given by Eq. (A4). the modified program which has been applied to the three-mode analysis is used with the orders of AR and MA parts being set to 4 and 3, respectively. Table A1 shows the frequency range (f_L, f_U) and ratios of the estimated-to-true values of the AR coefficients and modal parameters. Agreement between the estimated and true values of the AR coefficients are quite good for both cases. Even though the frequencies are spaced very closely, the modes can be separated with considerable accuracy.

Finally, it is recommended in a practical application that the estimation should consist of preliminary and main analyses. The preliminary analysis is made on a basis of a crude selection of the band pass range. But the estimated frequencies f_j can be expected to be relatively accurate since the band range has a small effect on the estimated values of frequency unless it is selected improperly. Hence, using the result of the first analysis, we may choose the frequency range more elaborately for the second estimation.

Table A1 Ratios (%) of the estimated-to-true values of the AR coefficients and modal parameters

Case	f_L[a]	f_U	$b(3)$	$b(2)$	$b(1)$	$b(0)$	f_1	f_2	η_1	η_2
I[b]	170	230	98	99	98	100	99	102	117	79
II	175	225	96	97	95	98	99	103	142	149

a) f_U and f_L: upper and lower frequencies of band pass filtering, respectively.

b) Case I: $f_1=190$ and $f_2=210$ Hz, Case II: $f_1=195$ and $f_2=205$ Hz.

REFERENCES

1 Coupry, G., "Random Techniques for Flutter Testing in Wind Tunnel and in Flight," Israel Journal of Technology, Vol. 11, March 1973, pp. 33–39.

2 Houbolt, J. C., "Subcritical Flutter Testing and System Identification," NASA CR-132480, Aug. 1974.

3 Natke, H. G., "Survey of European Ground and Flight Vibration Test Methods," SAE Report 760878, 1976.

4 Zimmerman, N. H., and Weissenburger, J. T., "Prediction of Flutter Onset Speed Based on Flight Testing at Subcritical Speeds," Journal of Aircraft, Vol. 1, July-Aug. 1964, pp. 190–202.

5 Brignac, W. J., Ness, H. B., and Smith, L. M., "The Random Decrement Technique Applied to the YF-16 Flight Flutter Tests," AIAA Paper No. 75–776, May 1975.

6 Dobbs, S. K., and Hodson, C. H., "Determination of Subcritical Frequency and Damping From B-1 Flight Flutter Test Data," NASA Contractor Report 3152, June 1979.

7 Abla, M. A., "The Application of Recent Techniques in Flight Flutter Testing," NASA SP-415, Proceedings of Conference held at Dryden Flight Research Center, Edwards, Calif., Oct. 1975, pp. 395–411.

8 Huttsell, L. J., Noll, T. E., and Holsapple, D. E., "Wind Tunnel Investigation of Supersonic Wing-Tail Flutter," NASA SP-415, Proceedings of Conference held at Dryden Flight Research Center, Edwards, Calif., Oct. 1975, pp. 193–211.

9 Foughner, J. T., Jr., "Some Experience Using Subcritical Response Methods in Wind-Tunnel Flutter Model Studies," NASA SP-415, Proceedings of Conference held at Dryden Flight Research Center, Edwards, Calif., Oct. 1975, pp. 181–191.

10 Stepner, D. E., and Mehra, R. K., "Maximum Likelihood Identification and Optimal Input Design for Identifying Aircraft Stability and Control Derivatives," NASA CR-2200, March 1973.

11 Mehra, R. K., Stepner, D. E., and Tyler, J. S., "Maximum likelihood Identification of Aircraft Stability and Control Derivatives," Journal of Aircraft, Vol. 11, Feb. 1974, pp. 81–89.

12 Bennett, R. M., Farmer, M. G., Mohr, R. L., and Hall, W. E., Jr., "Wind-Tunnel Technique for Determining Stability Derivatives from Cable-Mounted Models," Journal of Aircraft, Vol. 15, May 1978, pp. 304–310.

13 Murthy, H. S., Jategaonkar, R. V., and Balakrishna, S., "Dynamic Stability Measurements from Tunnel Unsteadiness Excited Random Response," Journal of Aircraft, Vol. 17, Jan. 1980, pp. 7–12.

14 Onoda, J., "Estimation of Dynamic Charactreistics of a Wing from the Random Response to Turbulence (in Japanese)," Journal of the Japan Society for Aeronautical and Space Sciences, Vol. 26, Dec. 1978, pp. 649–656.

15 Akaike, H., "Statistical Prediction Identification," Annals of the Institute of Statistical Mathematics, Vol. 22, 1970, pp. 203–217.

16 Box, G. E. P., and Jenkins, G. M., Time Series Analysis—Forecasting and Control, Holden Day, San Francisco, 1970.

17 Akaike, H., Arahata, E., and Ozaki, T., "TIMSAC-74, A Time Series Analysis and Control Program Package-(1)," Computer Science Monographs, No. 5, The Institute of Statistical Mathematics, Tokyo, March 1975.

18 Akaike, H., "Canonical Correlation Analysis of Time Series and the Use of an Information Criterion," System Identification—Advances and Case Studies, R. K. Mehra and D. G. Lainiotis, eds., Academic Press, New York, 1976, pp. 27–96.

19 Jury, I. E., Theory and Application of the z-Transform Method, John Wiley, New York, 1964.

20 Frazer, R. A., Duncan, W. J., and Collar, A. R., Elementary Matrices and Some Applications to Dynamic and Differential Equations, Cambridge University Press, London, 1938.

21 Jury, E. I., and Pavlidis, T., "Stability and Aperiodicity Constraints for System

Design," IEEE Transactions on Circuit Theory, Vol. CT-10, March 1963, pp. 137–141.

22 Irwin, C. A. K., and Guyett, P. R., "The Subcritical Response and Flutter of a Swept-Wing Model," ARC R. & M. No. 3497, 1965.

23 Gersh, W., and Sharpe, D. R., "Estimation of Power Spectra with Finite-Order Autoregressive Models," IEEE Transactions on Automat. Contr., Vol. AC-18, 1973, pp. 367–369.

24 Wilcox, P. R., and Crawford, W. L., "A Least Squares Method for the Reduction of Free-Oscillation Data," NASA TN D-4503, 1968.

25 Katz, H., Foppe, F. G., and Grossman, D. T., "F-15 Flight Flutter Test Procedure," NASA SP-415, Proceedings of Conference held at Dryden Flight Research Center, Edwards, Calif., Oct. 1975, pp. 413–431.

TECHNICAL REPORT OF NATIONAL
AEROSPACE LABORATORY
TR-667T

航空宇宙技術研究所報告667T号(欧文)

昭和56年4月発行

発行所 航空宇宙技術研究所
東京都調布市深大寺町1880
電話武蔵野三鷹(0422)47-5911(大代表)〒182
印刷所 株式会社 東京プレス
東京都板橋区桜川2－27－12

Published by
NATIONAL AEROSPACE LABORATORY
1,880 Jindaiji, Chōfu, Tokyo
JAPAN